

Electronic Supplementary Information for

Ligand-to-Metal Ratio Controlled Assembly of Nanoporous Metal-Organic Frameworks

Jian-Guo Lin,^a Yan-Yan Xu,^a Ling Qiu,^b Shuang-Quan Zang,^a Chang-Sheng Lu,^a Yi-Zhi Li,^a Song Gao,^c and Qing-Jin Meng^{*a}

^a *Coordination Chemistry Institute, State Key Laboratory of Coordination Chemistry, School of Chemistry and Chemical Engineering, Nanjing University, Nanjing 210093, China.*

^b *Key Laboratory of Nuclear Medicine, Ministry of Health, Jiangsu Institute of Nuclear Medicine, Wuxi 214063, China.*

^c *Beijing National Laboratory for Molecular Sciences, College of Chemistry and Molecular Engineering, Peking University, Beijing 100871, China.*

* To whom correspondence should be addressed. E-mail: mengqj@nju.edu.cn.

Syntheses of **1** and **2**

A single crystal of **1** was prepared by treating $\text{Cd}(\text{NO}_3)_2 \cdot 6\text{H}_2\text{O}$ (0.1 mmol), 1,3-Benzenedicarboxylic acid (0.05 mmol), and TPT (0.05 mmol) in water (6 mL) by the hydrothermal technique in a teflon-lined autoclave. In the course of the preparation, the pH value of the aqueous mixture was pre-adjusted to about 6 with 0.01 M NaOH aqueous solution. The autoclave was heated under autogenous pressure to 160 °C for 3 days and then cooled to RT over 24 h. Upon cooling the mixture to RT, the desired product appeared as long colourless rectangular parallelepipeds in ca. 61% yield (based on TPT). Elemental analysis (%) calcd for $\text{C}_{32}\text{H}_{32}\text{CdN}_4\text{O}_{10}\text{S}$ (777.08): C 49.46, H 4.15, N 7.21%; found: C 49.61, H 4.01, N 7.36%.

Compound **2** was synthesized by using the same method as for **1**, but only the amount of 1,3-Benzenedicarboxylic acid was up to 0.1 mmol. Yield ca. 56%. Elemental analysis (%) calcd for $\text{C}_{40}\text{H}_{26}\text{CdN}_4\text{O}_8\text{S}$ (835.11): C 57.53, H 3.14, N 6.71%; found: C 57.36, H 3.39, N 6.52%.

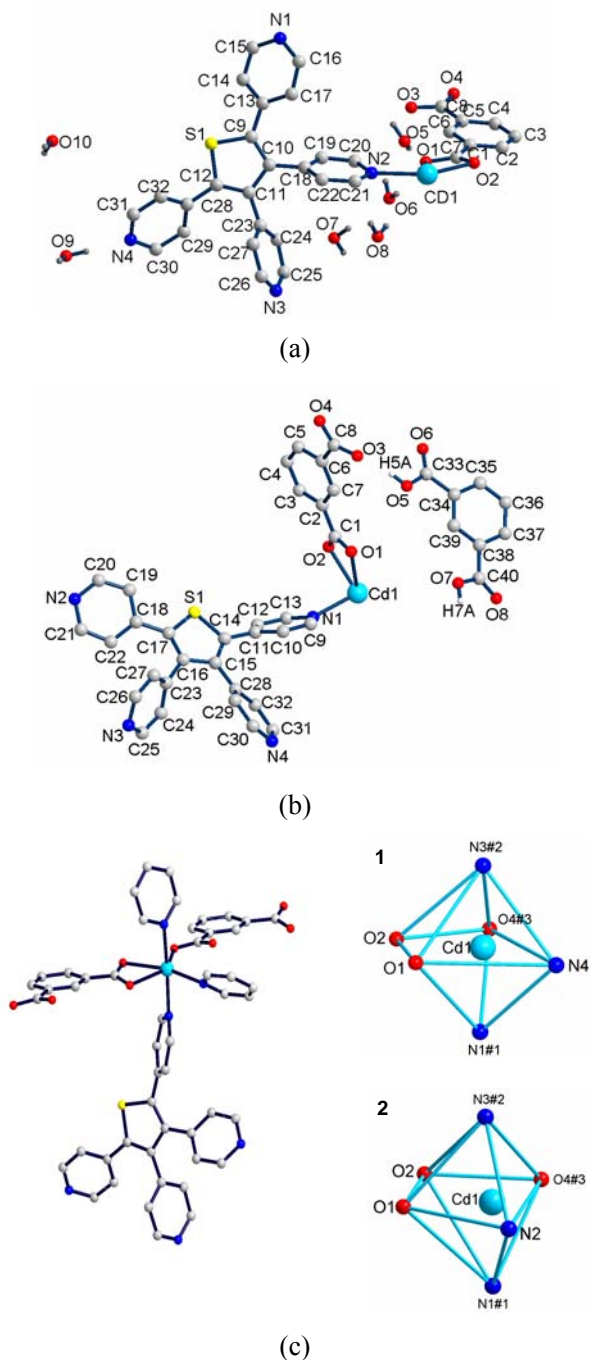


Fig. S1 (a) The asymmetrical unit of **1**. (b) The asymmetrical unit of **2**. (c) Coordination geometry of the Cd^{2+} ions in **1** and **2**. Symmetry codes: **1**: #1 = 0.25+x, 0.75-y, -0.25+z; #2 = -0.25+x, 0.75-y, 0.25+z; #3 = x, y, -1+z; **2**: #1 = x, -1+y, z; #2 = 1-x, -0.5+y, 0.5-z; #3 = 1+x, y, z.

The central cadmium(II) ions in **1** and **2** are in the same distorted octahedral coordination sphere, which are defined by two TPT nitrogen donor occupying the axial positions. While the equatorial positions are furnished by one TPT nitrogen atom, one mono(bidentate) and monodentate carboxylate oxygen atoms from two different BDC^{2-} ligands.

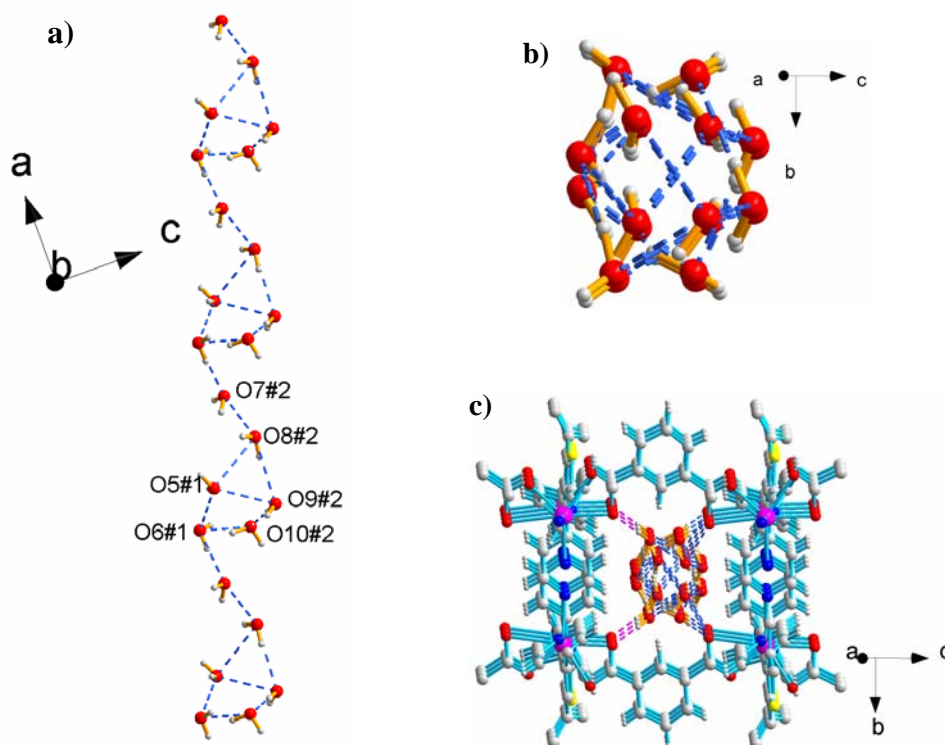


Fig. S2 (a) and (b) The 1-D water chain viewed in different directions. Hydrogen bonds are marked as dashed line. (c) Perspective view of the nanosized host channel embodying a guest water chain and the hydrogen-bond interactions between the guest and host molecules. Hydrogen bonds are marked as dashed lines. The detailed geometry parameters for hydrogen bonds are summarized in Table S1.

Table S1. Geometry Parameters for Hydrogen Bonds in **1**.

D-H	d(D-H)	d(H...A)	<DHA	d(D...A)	A
O(5)-H(5C)	0.85	2.210	130.36	2.834	O(6)
O(6)-H(6D)	0.85	1.830	169.00	2.668	O(7)
O(7)-H(7A)	0.85	2.112	130.58	2.742	O(8)
O(8)-H(8B)	0.85	2.429	112.59	2.866	O(5)#1
O(8)-H(8D)	0.85	2.020	163.00	2.843	O(9)
O(9)-H(9B)	0.85	2.500	106.00	2.854	O(5)#1
O(10)-H(10A)	0.85	1.960	177.00	2.810	O(6)#1
O(5)-H(5D)	0.85	1.900	179.00	2.668	O1
O(7)-H(7C)	0.85	2.160	145.00	2.899	N4#2
O(10)-H(10A)	0.85	1.960	177.00	2.810	O3#1

Symmetry codes: #1 $1/4+x, 3/4-y, -1/4+z$; #2 $3/4-x, -1/4+y, 1/4+z$

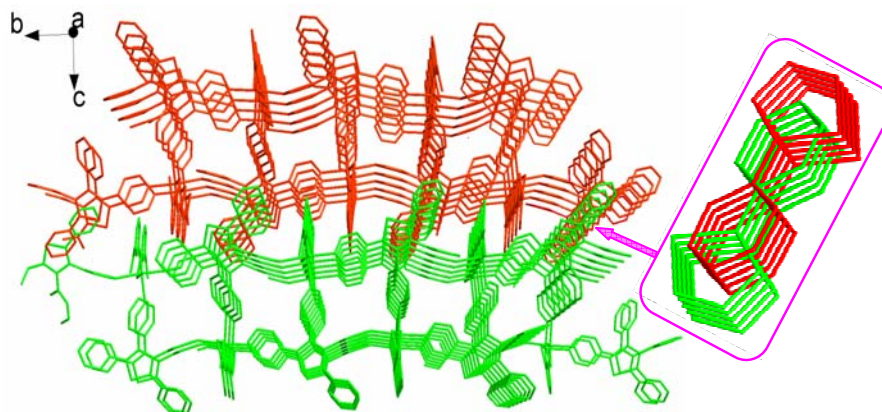


Fig. S3 The 3-D supermolecular network of **1** with the $\pi \cdots \pi$ interactions between the thiophene and pyridine rings.

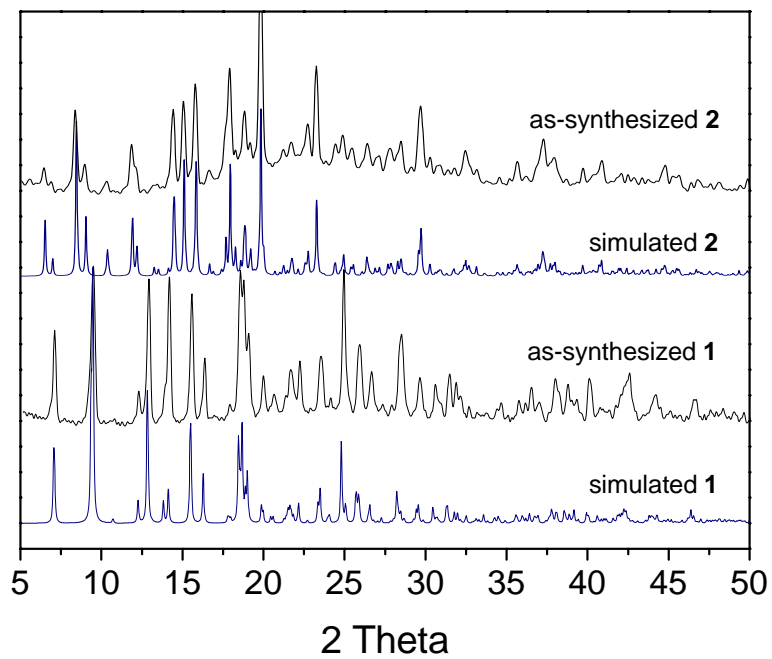


Fig. S4 The PXRD for as-synthesized and simulated of **1** and **2**.

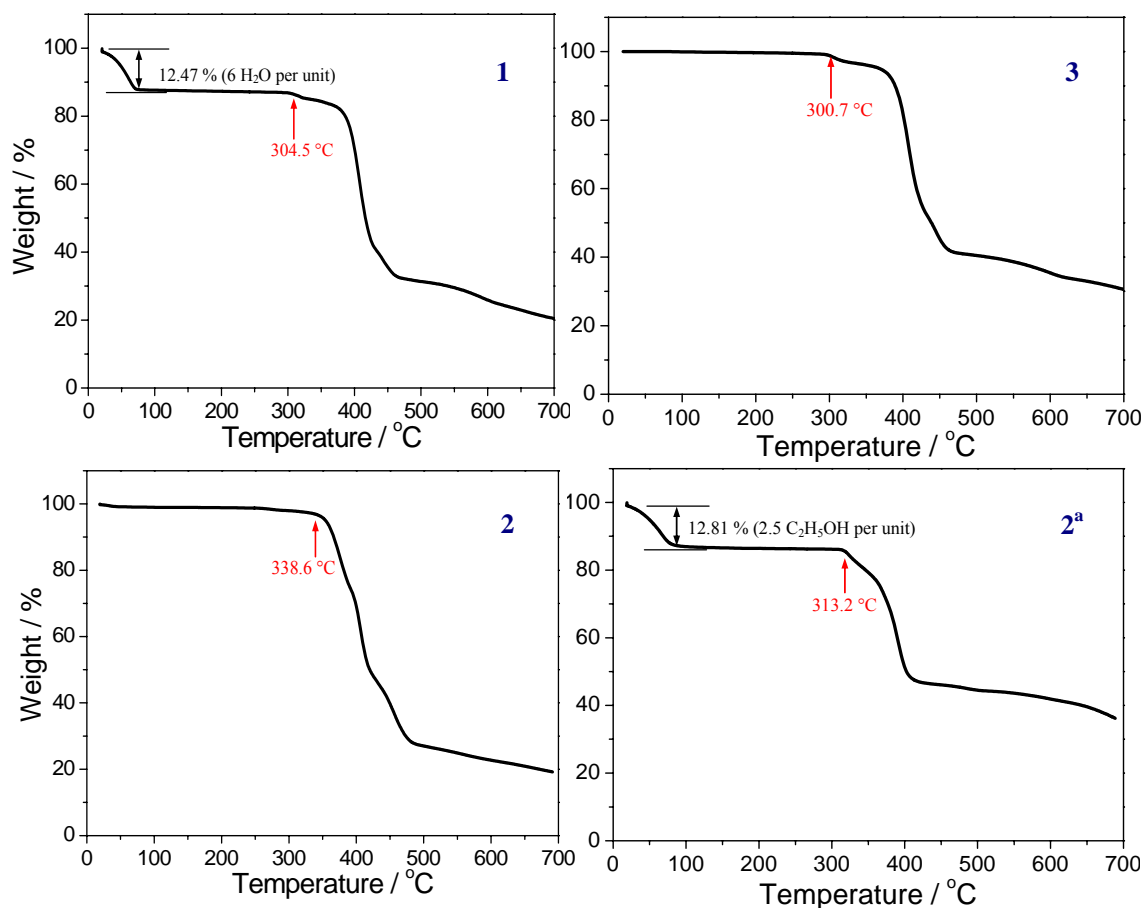


Fig. S5 Thermogravimetric analysis (TGA) for complexes **1**, **2**, **2^a**, and **3**, respectively.

TGA of complex **2** reveals that there is no weight loss below 330 °C. Over this temperature, a weight loss step between 330 °C and 420 °C was observed and attributed to the decomposition of solid H₂BDC along with the framework. The fact that the free H₂BDC is not easy to be removed from the host network may be attributed to the following two reasons: (i) the guest H₂BDC is rigid and spatially complementary to the vacant cavities of the MOF; (ii) the existence of strong hydrogen bonds between the host and guest molecules. TGA of complex **2^a** indicates a weight loss of 13.11% (calculated 12.89%) occurred below 110 °C, corresponding to the removal of two and a half ethanol molecules per formula unit, then followed by a plateau region from 110 to 330 °C. Beyond this temperature, a weight loss step between 330 °C and 400 °C was observed and attributed to the decomposition of the framework.

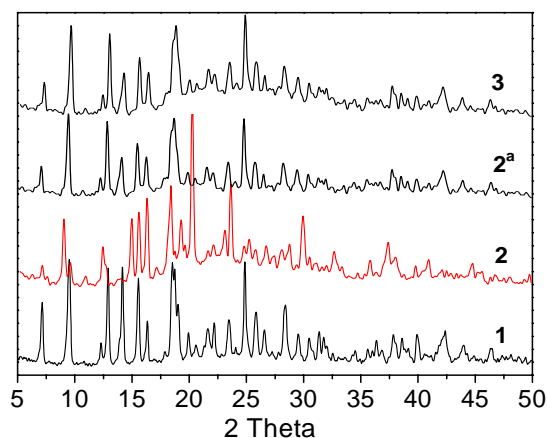


Fig. S6 Powder XRD patterns for as-synthesized **1**, **2**, **2^a**, and **3**, respectively.

Notably, the reason that intensity, width and position of some peaks in the recorded PXRD of **2** have minor difference with the others may be ascribed to the shape and size of the channels and the relative arrangements of bilayers being subject to a subtle change when it encapsulated H₂BDC molecules. This result is consistent with the single-crystal X-ray structure determination.

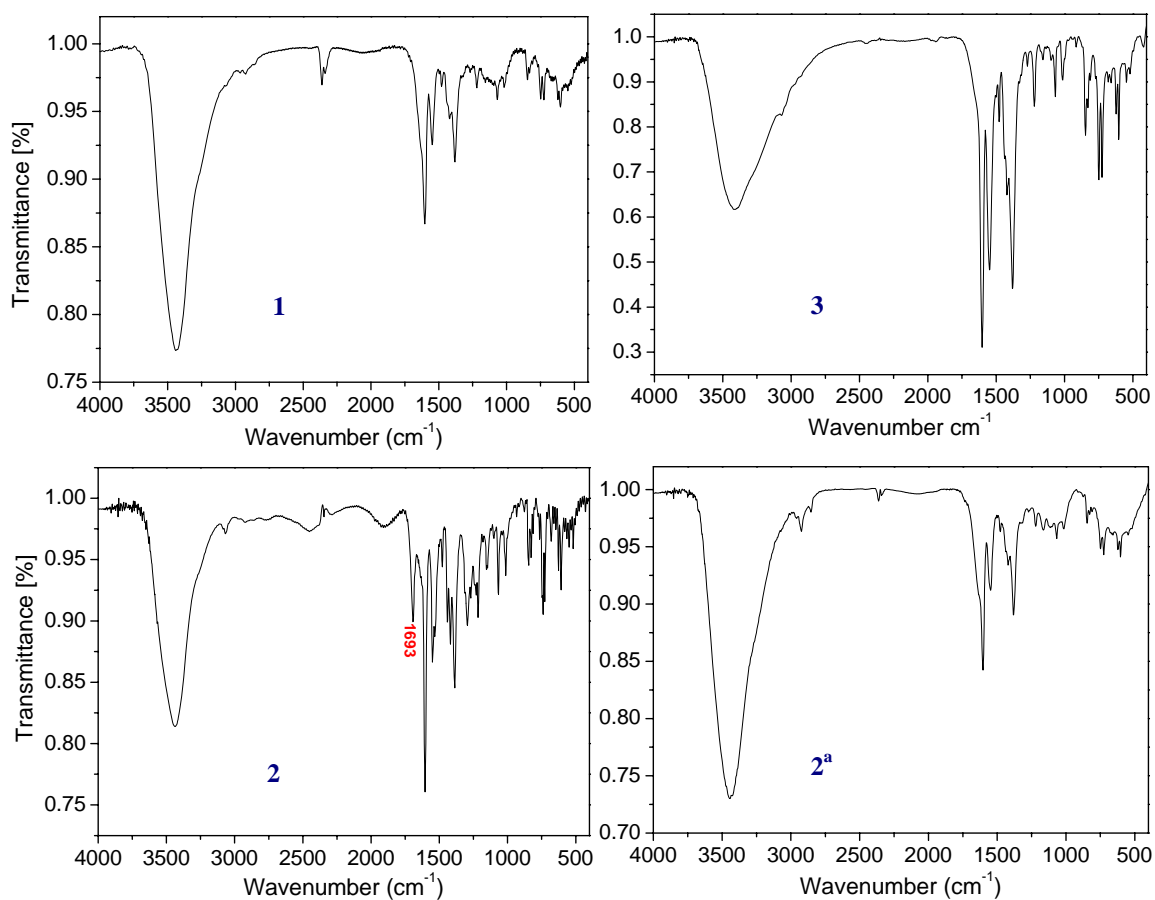


Fig. S7 IR spectra of the complexes. FT-IR (KBr): The characteristic absorption peak at $\nu = 1693$ (cm⁻¹) indicate the appearance of the carboxyl group from free H₂BDC molecule.

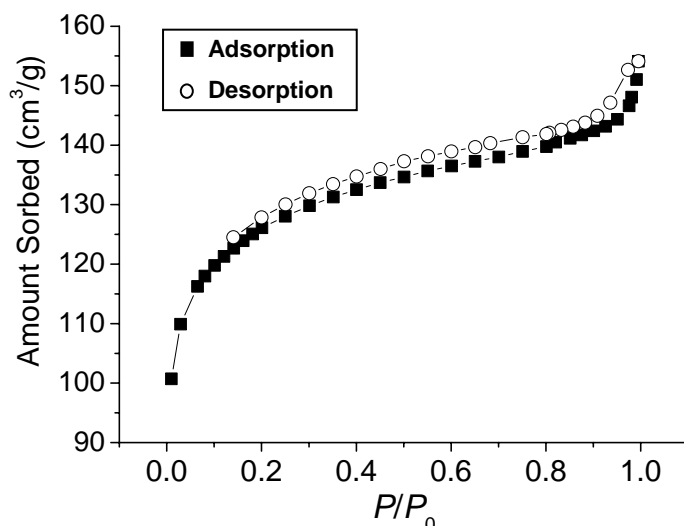


Fig. S8 Adsorption/desorption isotherm of nitrogen gas (77 K) for 3.

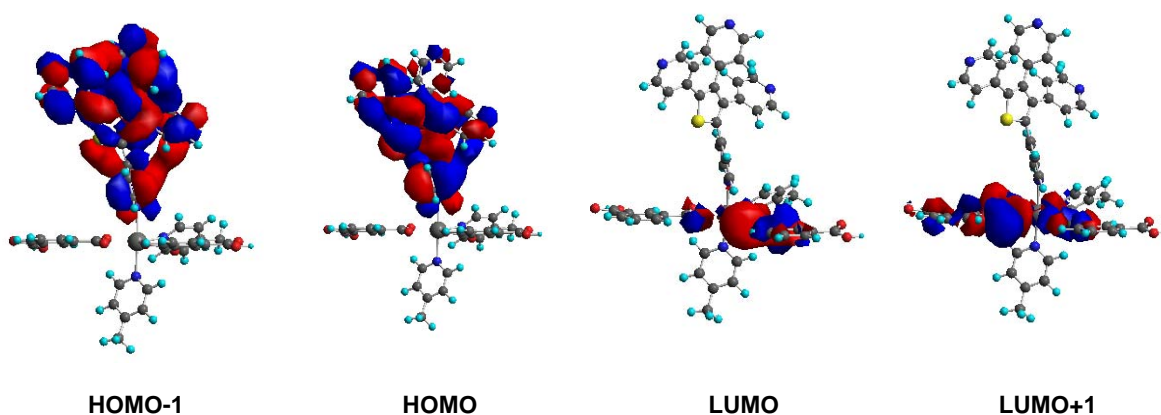


Fig. S9 The electron-density distribution of the corresponding frontier molecular orbitals calculated for the framework.

The related mononuclear specie $[\text{Cd}(\text{BDC})_2(\text{mp})_2(\text{TPT})]^{2-}$ (mp = γ -methylpyridine) ground-state geometry adapted from the truncated X-ray data were used to calculate and evaluate their electronic structure and ground-state properties. To evaluate the absorption spectra of the complexes and to verify the nature of the molecular orbitals involved in the absorption and emission processes, density functional theory (DFT) calculations on the electronic ground states and time-dependent DFT calculations in the singlet states were carried out by the Gaussian 03 program^[1] with the B3LYP hybrid functional.^[2] “Double- ξ ” quality basis set LANL2DZ, which uses Duning D95V basis set on first row atoms and Los Alamos ECP plus DZ on Na-Bi, was employed as the basis set. This has been proved to be useful and satisfactory for other metal polypyridyl complexes according to the literatures.^[3]

All calculations were performed on a Pentium-IV personal computer using the default convergence criteria given in the program. The results indicate that the lowest singlet excitation for the framework is dominated by the approximately degenerate combination of HOMO \rightarrow LUMO and HOMO \rightarrow LUMO+1 transitions, in which HOMO are mostly composed of π orbitals of thiophene and pyridine rings of TPT ligand and both LUMO and LUMO+1 mainly consist of π^* orbitals of benzene rings of the H₂BDC ligands (Figure S8). As a result, the origin of the fluorescences at 397-427 nm of these complexes can be ascribed to ligand-to-ligand charge transfer (LLCT).

References:

- [1] Frisch, M. J.; Trucks, G. W.; Schlegel, H. B.; Scuseria, G. E.; Robb, M. A.; Cheeseman, J. R.; Montgomery, J. A.; Vreven, T.; Kudin, K. N.; Burant, J. C.; Millam, J. M.; Iyengar, S. S.; Tomasi, J.; Barone, V.; Mennucci, B.; Cossi, M.; Scalmani, G.; Rega, N.; Petersson, G. A.; Nakatsuji, H.; Hada, M.; Ehara, M.; Toyota, K.; Fukuda, R.; Hasegawa, J.; Ishida, M.; Nakajima, T.; Honda, Y.; Kitao, O.; Nakai, H.; Klene, M.; Li, X.; Knox, J. E.; Hratchian, H. P.; Cross, J. B.; Bakken, V.; Adamo, C.; Jaramillo, J.; Gomperts, R.; Stratmann, R. E.; Yazyev, O.; Austin, A. J.; Cammi, R.; Pomelli, C.; Ochterski, J. W.; Ayala, P. Y.; Morokuma, K.; Voth, G. A.; Salvador, P.; Dannenberg, J. J.; Zakrzewski, V. G.; Dapprich, S.; Daniels, A. D.; Strain, M. C.; Farkas, O.; Malick, D. K.; Rabuck, A. D.; Raghavachari, K.; Foresman, J. B.; Ortiz, J. V.; Cui, Q.; Baboul, A. G.; Clifford, S.; Cioslowski, J.; Stefanov, B. B.; Liu, G.; Liashenko, A.; Piskorz, P.; Komaromi, I.; Martin, R. L.; Fox, D. J.; Keith, T.; Al-Laham, M. A.; Peng, C. Y.; Nanayakkara, A.; Challacombe, M.; Gill, P. M. W.; Johnson, B.; Chen, W.; Wong, M. W.; Gonzalez, C.; Pople, J. A. *Gaussian 03*; Gaussian, Inc.: Wallingford, CT, **2004**.
- [2] a) Becke, A. D. *J. Chem. Phys.* **1993**, *98*, 5648; b) Lee, C.; Yang, W.; Parr, R. G. *Phys. Rev. B* **1988**, *37*, 785.
- [3] a) Yong, L.; Hoffmann, S. D.; Fässler, T. F.; Riedel, S.; Kaupp, M. *Angew. Chem., Int. Ed. Engl.* **2005**, *44*, 2092; b) Zheng, S.-L.; Yang, J.-H.; Yu, X.-L.; Chen, X.-M.; Wong, W.-T. *Inorg. Chem.* **2004**, *43*, 830; c) Liu, X.; Guo, G. C.; Fu, M. L.; Liu, X. H.; Wang, M. S.; Huang, J. S. *Inorg. Chem.* **2006**, *45*, 3679.